Conf-910591--1

RESIDUAL STRESS CALCULATIONS IN WHISKER-REINFORCED CERAMIC MATRIX COMPOSITES

Zhuang Li
Materials Science Division
Argonne National Laboratory, Argonne, IL 60439-4838

Richard C. Bradt
Mackay School of Mines
University of Nevada-Reno, Reno, Nevada 89557-0047

Received by OSTI
MAY 06 1991

ANL/CP--72402

DE91 011163

February 1991

The submitted manuscript has been authored by a contractor of the U.S. Government under contract No. W-31-109-ENG-38. Accordingly, the U.S. Government retains a nonexclusive, royalty-free license to publish or reproduce the published form of this contribution, or allow others to do so, for U.S. Government purposes.

DISCLAIMER

This report was prepared as an account of work sponsored by an agency of the United States Government. Neither the United States Government nor any agency thereof, nor any of their employees, makes any warranty, express or implied, or assumes any legal liability or responsibility for the accuracy, completeness, or usefulness of any information, apparatus, product, or process disclosed, or represents that its use would not infringe privately owned rights. Reference herein to any specific commercial product, process, or service by trade name, trademark, manufacturer, or otherwise does not necessarily constitute or imply its endorsement, recommendation, or favoring by the United States Government or any agency thereof. The views and opinions of authors expressed herein do not necessarily state or reflect those of the United States Government or any agency thereof.

Submitted to the ASM International "Proceeding on Practical Applications of Residual Stress Technology Conference," Indianapolis, IN, May 15-17, 1991.

---

*Work supported by the U.S. Department of Energy, BES-Materials Sciences, under contract #W-31-109-ENG-38.

MASTER

DISTRIBUTION OF THIS DOCUMENT IS UNLIMITED

Residual Stress Calculations in Whisker-Reinforced Ceramic Matrix Composites

by

Zhuang Li* **and Richard C. Bradt+**

*Materials Science Division
Argonne National Laboratory**, Argonne, IL 60439

+Mackay School of Mines
University of Nevada - Reno, Reno, NV 89557-0047

Submitted to the ASM International "Proceeding on Practical Applications of Residual Stress Technology Conference," 15-17 May 1991, Hyatt Regency, Indianapolis, IN.

**Work supported by the U.S.Department of Energy, Basic Energy Sciences-Materials Sciences under Contract #W-31-109-ENG-38.

Residual Stress Calculations in Whisker-Reinforced Ceramic Matrix Composites

by

Zhuang Li* and Richard C. Bradt+

*Materials Science Division
Argonne National Laboratory**, Argonne, IL 60439

+Mackay School of Mines
University of Nevada - Reno, Reno, NV 89557-0047

**Work supported by the U.S.Department of Energy, Basic Energy Sciences-Materials Sciences under Contract #W-31-109-ENG-38.

Residual Stress Calculations in Whisker-Reinforced Ceramic Matrix Composites

by

Zhuang Li* **and Richard C. Bradt+**

*Materials Science Division
Argonne National Laboratory, Argonne, IL 60439

+Mackay School of Mines
University of Nevada - Reno, Reno, NV 89557-0047

Abstract

By using a modified Eshelby method, the residual stresses in SiC whisker/alumina matrix and sapphire whisker/mullite matrix composites have been calculated. The results indicate that significant residual stresses are present and are in good agreement with independent experimental measurements. Four factors are observed to influence the magnitudes and distributions of the residual stresses in these multiphase composites. They are: (i) the thermal expansion mismatch, $\Delta\alpha$, (ii) the elastic modulus mismatch, ΔE, (iii) the geometry, (L/d) ratio, of the reinforcing phase and (iv) the concentration or volume fraction of the reinforcing phase.

I. Introduction

Almost since ceramics have been applied for utilitarian purposes, residual stresses in ceramics have been incorporated as a design parameter to improve their strength. Fine ceramic glazes with thermal expansions less than those of the underlying body are familiar to most, as cracked glazes frequently occur when the glaze is not under a sufficient level of compression. Ancient Chinese and Japanese potters took advantage of this cracking to develop the famous "crackle-glaze" patterns, which are now prized by many collectors of fine porcelains centuries after their initial development. Surface compressive stresses to strength glass objects are now commonplace as most structural glass panels are tempered to enhance their strength and improve their safety. The latter, a consequence of the high strain energy density in the tempered glass, results because the fracture pattern of tempered glass is one of harmless, small. equiaxed fragments as opposed to dangerous, large, lance-like fracture pieces of dead-annealed glass. Materials scientists who are familiar with ceramics and glasses are thoroughly appraised of the above residual stress situations.

Recently, materials scientists have developed ceramic matrix composites (CMC's) with ceramic reinforcing phases that present a unique and interesting situation of residual stresses. Because both constituents are "brittle" ceramics, there is little opportunity for annealing or stress relaxation to occur when these ceramic reinforced-ceramic matrix composites (CMC's) are cooled from their processing (synthesis) temperatures, often above 1000°C. This has the tendency to develop very high residual stresses because of the large ΔT on cooling from processing. Equally interesting is the feature that the reinforcing phase of these CMC's, be it a whisker or a particle, is usually a single crystal. This introduces the complications of anisotropic elasticity and anisotropic thermal expansion into the phenomenon, but their accompanying benefits as well. As single crystals often possess elastic moduli that may vary considerably with crystallographic orientation (a factor of two is not uncommon) and thermal expansions can be equally anisotropic, it is evident that significant residual stresses will be present in these composites.

This paper addresses those residual stresses from a fundamental perspective, presenting an Eshelby-type model for their theoretical calculation. After developing the model, it is applied to several composite systems of current interest, including silicon carbide reinforced aluminum oxide and sapphire whisker reinforced mullite

II. Formulation of Residual Stress Calculations

Studies of the residual stresses in multiphase composites have been in progress for several decades. Numerous models have been proposed; however, among those various models, it is the modifications of the Eshelby method [1-3] which appear the most promising. This is because the Eshelby approach can exactly solve the stress field of a single crystal second phase inclusion and is also relatively easy to apply to actual crystalline systems. Using the modified Eshelby method, the following residual stress problems in composites can be directly addressed: (i) stresses within an anisotropic single crystalline second phase inclusion, (ii) the stresses at the interface between a second phase inclusion and the matrix, (iii) the average stress within the matrix, (iv) the effect of the geometry of the inclusion, (v) the effect of the inclusion volume fraction or concentration and (vi) the change of stresses within the reinforcing phase inclusion and the matrix by applied external stresses[4,5].

Fig. 1 schematically illustrates an ellipsoidal inclusion within a matrix. The thermal expansions and the elastic properties of the inclusion are considered to be as anisotropic while those of the matrix are assumed to be isotropic. The descriptive geometric parameters of the ellipsoidal inclusion are denoted as L and d, where L is specified as parallel to the X_3 axis of the inclusion and d coincides with the X_1 and X_2 axes. The angle ψ in Fig. 1 is the angle between the X_1 axis and the direction of interest. Two locations in the matrix just outside of the inclusion are of special interest. One is at the equator of the inclusion, $\psi=0^o$, as denoted by point B and the other is at the pole of the inclusion, $\psi=90^o$, as denoted by point A. If the (L/d) ratio of the inclusion is equal to unity, then the ellipsoidal inclusion is a spherical grain. For an (L/d) ratio much less than one, the inclusion is a flat tabular plate, and when the (L/d) ratio is much greater than unity the inclusion approximates a whisker. Those three special geometric shapes of the inclusion are also illustrated in Fig. 1 along the side of the schematic.

Details of the mathematical formulation of the micromechanical stress calculations can be found in several references[2-7] and are presented only in the final matrix form here. To determine the internal stresses it is necessary to solve for the eigenstrain, ε^*_{ij}, which is generated by the thermal expansion and elastic moduli differences between the reinforcing phase inclusion and matrix. The eigenstrain of the inclusion is expressed as[4]:

$$[<C^D><S> + <C^M> - V_f<C^D><\bar{S}>]<\varepsilon^*> = <C^I><\varepsilon^T> - <C^D><\varepsilon^o>, \qquad (1)$$

where the $<C^I>$, $<C^M>$ and $<C^D>$ are each 6x6 matrices of the elastic stiffnesses for the inclusion, the matrix, and the difference between the inclusion and the matrix, respectively. The $<S>$ and $<\bar{S}>$ are each 6x6 matrices of the Eshelby tensor and the average Eshelby tensor, respectively. These are directly related to the geometry of the inclusion and the elastic properties of the matrix. The V_f is the volume fraction of the inclusion. The $<\varepsilon^o>$, $<\varepsilon^T>$ and $<\varepsilon^*>$ are each 6x1 matrices of the applied strain, the thermal strain and the eigenstrain, respectively. The ε^o_{ij} and ε^T_{ij} are given by:

$$\varepsilon^o_{ij} = (C^M_{ijkl})^{-1}\sigma^o, \tag{2a}$$

and

$$\varepsilon^T_{ij} = (\alpha^I_{ij} - \alpha^M)\Delta T, \tag{2b}$$

where the $(C^M_{ijkl})^{-1}$ is the elastic compliance of the matrix. The σ^o_{ij} is the applied stress and the α^I_{ij} and α^M, respectively, are the thermal expansions of the inclusion and matrix. The ΔT is the temperature difference. Eq. 1 can be considered to be the basic equation for the microstructural design of ceramic matrix composites on a mechanics basis.

The stresses inside of the reinforcing phase inclusion can then be calculated as:

$$<\sigma^{in}> = <\sigma^o> + <C^M>[<S> - <I> - V_f<\bar{S}>]<\varepsilon^*>, \tag{3}$$

While the average stress in the composite matrix is determined from:

$$<\sigma^M> = <\sigma^o> - V_f<C^M><\bar{S}><\varepsilon^*>. \tag{4}$$

The stresses just outside of the inclusion at the interface are expressed by:

$$<\sigma^{out}> = <\sigma^{in}> - <C^M><B><C^M><\varepsilon^*> + <C^M><\varepsilon^*>, \qquad (5)$$

where <I> is a 6x6 identity matrix and <B> is a 6x6 matrix related to the elastic constants of the matrix and the unit vector outward from the inclusion[4].

From the above equations it is evident that the eigenstrain, ε^*_{ij}, is directly related to the internal micromechanical stresses. The eigenstrain and thus the residual stresses are influenced by the following four parameters: (i) the matrix - inclusion thermal expansion difference, $\Delta\alpha$, (ii) their elastic moduli difference, ΔE, (iii) the geometry of the reinforcing phase inclusion, or its aspect ratio, (L/d), and (iv) the volume fraction of the reinforcing phase inclusion, V_f. The relationships between the eigenstrain and those four factors are clearly illustrated through the Eq. 1. The first and second terms on the right hand side of Eq. 1, respectively, indicate the effects of $\Delta\alpha$ and ΔE on the residual stresses. On the left hand side of Eq. 1 the <S> and V_f, respectively, indicate the effects of the geometry of the reinforcing inclusion, (L/d), and the concentration of the inclusions on the residual stresses.

Eqs. 1-5 indicate that although the residual stresses are highly dependent on the inclusion shape, they are independent of the inclusion size. Many experimental results, however, show that the inclusion or individual particle size can greatly influence the mechanical properties of ceramic materials, such as strength, fracture toughness, etc.. Davidge and Green[8] and Kuszyk and Bradt[9] have clearly demonstrated the relationship between the microcracking and the inclusion or grain size of a particular composite or non-cubic polycrystalline ceramic. They proposed that when the strain energy of the inclusion or grain is larger than the surface energy required to form cracks, then microcracking will occur inside the materials. Therefore, it is necessary to calculate the strain energy induced by the thermal and elastic mismatch within the composites. The formulation of the strain energy can also be readily derived from the modified Eshelby method[3]. In matrix form[4] it can be expressed as:

$$\begin{aligned} W &= W^{o} + W^{*} + W^{T} \\ &= W^{o} + (1/2)V\langle\sigma^{o}\rangle[\langle\varepsilon^{*}\rangle - \langle\varepsilon^{T}\rangle] - (1/2)V[\langle\sigma^{in}\rangle - \langle\sigma^{o}\rangle]\langle\varepsilon^{T}\rangle, \qquad (6) \end{aligned}$$

where the W^{o} is the strain energy generated from the applied stress, the W^{*} is due to the inhomogeneity of the inclusion and the W^{T} is the thermal strain energy of the inclusion. The V is the volume of the inclusion . Since the stress and the strain can be determined from Eqs. 1-5, the strain energy can be readily calculated. In the absence any applied stress, if the thermoelastic properties of the inclusion are isotropic and the shape of the inclusion is a sphere, then Eq. 6 is identical to the formula derived by Davidge and Green□. It is evident from Eq. 6 that the strain energy is not only dependent on the inclusion size, but it is also dependent on the reinforcing phase inclusion shape, (L/d), because both the stress and strain are shape dependent.

III. Whisker Reinforced Ceramic Matrix Composites

By applying Eqs. 1-5 the residual stresses within SiC whisker reinforced polycrystalline alumina matrix composite and sapphire whisker reinforced polycrystalline mullite matrix composite were calculated. As illustrated in Fig. 1 the reinforcing phase (whisker) can be assumed to have an ellipsoidal shape. The L dimension is defined to be parallel to the whisker growth direction. The growth direction of SiC whiskers is the [111]. For sapphire two different types, A-type and C-type, growth orientation single crystal whiskers may be used as reinforcing phases. The A-type sapphire whisker has an axial orientation of $<1\bar{2}10>$ while the C-type whisker has the <0001> growth direction. The thermoelastic properties of the reinforcing single crystal whiskers are treated as anisotropic while those of the polycrystalline ceramic matrix are isotropic. The thermoelastic properties of those materials are list in Table 1[10,11].

a). SiC Whisker/Alumina Matrix Composite

Since the SiC whisker reinforced polycrystalline alumina matrix composite has been demonstrated to exhibit enhanced mechanical properties[12,13], there have been extensive studies of the residual stresses of this materials[4,14-17]. Fig. 2 illustrates the residual stresses for a single SiC inclusion within a polycrystalline alumina matrix as a function of the inclusion (L/d) ratio calculated from the previous equations. The stresses plotted in Fig. 2 are the stresses within the SiC whisker, σ^I_{ij}, the radial and tangential stresses, σ_{rr} and $\sigma_{\theta\theta}$, just outside inclusion in the matrix as illustrated in Fig. 1. The ΔT for the calculation is 1000°C, as on cooling from the composite processing temperature the stress relaxation by creep processes will occur until around 1000°C. Fig. 2 shows that the stresses within the SiC whisker σ^I_{ij} and the radial stresses σ_{rr} at the interface are in compression (a minus sign) while the tangential stresses $\sigma_{\theta\theta}$ at the interface are in tension. The magnitudes of those stresses are significantly high, in GPa range, and are highly dependent on the geometry of the inclusion the (L/d) ratio. When the shape of the SiC inclusion varies from a flat plate to a whisker, as the (L/d) ratio is increased from 0.1 to 10, the σ^I_{33} continuously increases in compression from -0.25 to -2.0 GPa, while σ^I_{11} decreases from -2 to -1 GPa. For the (L/d) ratio larger than about eight those stresses essentially remain constant. The tangential stresses at the interface are also dependent on the (L/d) ratio. As the (L/d) ratio increases, the $\sigma^B_{\theta\theta}$ decrease to zero while $\sigma^A_{\theta\theta}$ and σ^B_{22} increase. Since the magnitudes of the residual stresses are very high, it is possible to damage the materials, which have been discussed in detail in reference [4]. It should also be noted that since the compressive radial stress or clamp stress, σ^B_{rr}, at the interface are extremely high about 1 GPa, the SiC whisker and alumina matrix are tightly bonded by these mechanical stresses.

The effect of the volume fraction of the SiC reinforcing phase on the magnitude of the residual stresses can also be determined. Fig. 3 depicts the residual stresses as a function of the volume fraction, V_f, of the whisker (L/d = 10). As the V_f increase the compressive stresses within the whisker are decreased while the tangential stresses at the interface and the average stress in the alumina matrix are increased in tension. The average stress in the alumina matrix increases from zero at $V_f = 0$ to 400 MPa at $V_f = 0.3$. This indicates that the volume fraction of the reinforcing phase is also an important factor for microdesigning any promising ceramic matrix composite, for the V_f directly affects the residual stress levels.

As indicated previously, the residual stresses within SiC whisker reinforced alumina matrix composites have been experimentally determined by different researchers. Predecki et al[14,15] have measured the residual stresses with different volume fraction of SiC by the X-ray diffraction technique. Majumdar et. al [16] and Tome et. al [17] have also measured and analyzed the residual stresses by neutron diffraction techniques. Fig. 4 compares the residual stresses experimentally determined from X-ray diffraction with the theoretical calculations at different volume fractions of the reinforcing phase and shows an excellent agreement between the two independent studies, except for the stresses within the 10% V_f SiC whiskers. This discrepancy suggests that some stress relaxation processes may occur within the SiC whiskers, such as microcracking, or dislocation movement, because for the 10% SiC whisker composite the σ^I_{33} is about 2 GPa in compression, as illustrated in Fig. 3. However, since the magnitude of σ^I_{33} rapidly decrease as the V_f increases which is also clear in Fig. 3, stress relaxation may not be occur for V_f larger than 10% and the residual stress determined from experiment and theoretical calculation are essentially the same. Fig. 4 also indicates that no microcracking occur inside the alumina matrix even at $V_f = 0.29$, at which the average matrix stress σ^M is about 400 MPa.

The close agreement of the experimentally measured residual stresses and the theoretically calculated residual stresses is obvious in Fig. 4. It confirms the use of the previously outlined Equations (1) through (6) to calculate the residual stresses for whisker reinforce composites.

Furthermore, it illustrates that when the second phase (reinforcing phase) of a composite is a single crystal (whisker or other shape), then it is necessary to apply concepts of anisotropic elasticity to calculate the residual stresses associated with the second phase. While these concepts have been specifically applied to the example of SiC whiskers reenforcing a polycrystalline alumina matrix, it is obvious that they are also applicable to similar problems such as inclusions in steels and precipitates in age hardenable metal systems. The aforementioned fundamentals of the residual stress calculations are applicable whenever a single crystal inclusion is present.

b) Sapphire Whisker/Mullite Matrix Composite

Another ceramic whisker reinforced ceramic matrix composite of technical interest for its potential long term high temperature thermodynamic stability is that of sapphire whiskers reinforcing a polycrystalline mullite matrix. Not only are the two phases in chemical equilibrium to the melting temperature of mullite, > 1800°C, but the two phases are both oxides and thus stable in air. Unfortunately, the sapphire whiskers have a much higher thermal expansion than the mullite matrix and this will put the whiskers in tension. the residual stress state will be the opposite as the previously discussed system. There have not been any reported experimental measurements of the residual stresses in this CMC, but the close agreement of the experimental and theoretical results for the previous composite system suggests that calculations are sufficient to define the residual stresses.

Fig. 5 illustrates the residual stresses of a 25% V_f C-type whisker sapphire inclusion within mullite matrix composite as a function of the (L/d) ratio. In contrast to the SiC/alumina composite the stress within the sapphire whisker and radial stresses at interface are tensile while the tangential stresses at the interface and the average stress in the matrix are compressive. Those stresses are also highly dependent on the (L/d) ratio. When the sapphire inclusion becomes a whisker as the (L/d) = 10, the σ^I_{33} is about 1.4 GPa in tension while the σ^M is about 200 MPa in compression. The mechanically interfacial bonding stress, σ^B_{rr}, is lower, only about 200 MPa in tension. The residual stresses within A-type sapphire whisker reinforced mullite matrix composite are similar to those of C-type. However, since the thermal expansion along the $<1\bar{2}10>$ is lower than that along the <0001>, the magnitude of the residual stresses in A-type sapphire whiskers are lower than those in C-type whiskers. For 25% A-type sapphire whisker the stress within whisker, σ^I_{33}, is about 900 MPa in tension and the stress in the matrix, σ^M, is about 170 GPa in compression.

Mah et. al [18] have processed and measured the mechanical properties of sapphire reinforced mullite matrix composites. From the chemical stability point of view, mullite appear to be a very promising candidate materials for sapphire reinforced composites, as has been described by Mah et al [18]. The mechanically interfacial bonding stress in sapphire/mullite composite is also different from that in SiC/alumina composite. In the sapphire/mullite composite the clamped stress around the sapphire whisker is in tension and the average stress in the mullite matrix is in compression, while in the SiC/alumina composite the clamped stress is in compression and the average stress in alumina matrix is in tension. If the fracture toughness is primarily influenced by the interfacial properties of the ceramic composites, the fracture behavior of sapphire/mullite composite should be superior to that of

SiC/alumina composite. However, the experimental results[18] show that, unlike the SiC/alumina composites, the mechanical properties of sapphire/mullite composites are rather poor. The reason is illustrated in Fig. 5 as large residual tensile stresses exist inside the sapphire whiskers, which will damage (fracture) the reinforcing phase and result in composite failure. Li and Bradt have discussed the residual stress effect on the fracture toughness of ceramic composites[4,19]. In SiC/alumina composite, although the interfacial bonding stress is high which may not be favorable to the debonding, the large compressive stress inside the SiC whisker may inhabit crack propagation through the reinforcing phase and promote whisker bridging of crack faces in the following wake-region of a crack. Therefore, to design a promising composite material, the micromechanical stresses must be consider and understood.

IV. Summary and Conclusions

A modification of the Eshelby method for the calculation of residual stresses in composites containing single crystal reinforcing phases has been presented. It addresses the anisotropic characteristics of the reinforcing phases, both the elastic anisotropy and the thermal expansion anisotropy. Stresses in both the reinforcing phases and the matrix can be calculated. The resulting methodology reveals that four factors influence the magnitudes and distributions of the residual stresses in these multiphase composites. The four factors are: (i) the thermal expansion mismatch, $\Delta\alpha$, (ii) the elastic modulus mismatch, ΔE, (iii) the geometry of the reinforcing phase and (v) the concentration, or volume fraction of the reinforcing phase.

This model has been applied to several ceramic matrix composites, including SiC whiskers in a polycrystalline alumina matrix and sapphire whiskers in a mullite matrix. The results confirm that the residual stresses are indeed highly dependent on the microstructure, especially on the shape of the reinforcing phase microstructural constituents. For example, in the case of the SiC whiskers in the polycrystalline Al_2O_3 matrix, the whiskers are in a residual stress state of compression at room temperature. However, the longitudinal stress is highly dependent on the (L/d) ratio when the whiskers are short, that is for (L/d)<4. This is particularly significant for the residual compressive stress is in the 1-2 GPa range. For sapphire whiskers in a mullite matrix, very high tensile stresses are predicted, and these may lead to the fracture of the sapphire whiskers during cooling from the high fabrication temperatures.

The aforementioned theoretical results are compared with independent experimental methods for measurement of the residual stresses. It is concluded that an Eshelby-type of analysis that fully accounts for the anisotropic elastic constants and thermal expansions is necessary to achieve accurate residual stress calculations when the reinforcing phase are present in single crystal form.

References

[1].J.D.Eshelby, "The Determination of the Elastic Field of an Ellipsoidal Inclusion, and Related Problem," *Proc. Roy. Soc. London*, *Ser. A*, 241 376-396 (1967).

[2].A.G.Khachaturyan, pp. 226-240, in Theory of Structural Transformations in Solids, John Wiley & Sons, New York (1983).

[3].T.Mura, pp. 66-75, in Micromechanics of Defects in Solid, Martinus Nijhoff Publishers, The Hague, Netherlands, (1982).

[4].Z.Li and R.C.Bradt, "Micromechanical Stresses in SiC-Reinforced Al_2O_3 Composites," *J. Am. Ceram. Soc.*, **72**, 70-77 (1989).

[5].Z.Li and R.C.Bradt, "Thermoelastic Micromechanical Stresses Associated with a Large α-Silicon Carbide Grain in a Polycrystalline β-Silicon Carbide Matrix," *J. Am. Ceram. Soc.*, **72** 459-466 (1989).

[6].T.Mori and K.Tanaka, "Average Stress in Matrix and Average Elastic Energy of Materials with Misfitting Inclusions," *Acta Metall.*, **21**, 571-574 (1973).

[7].M.Taya, "On Stiffness and Strength of an Aligned Short Fiber Reinforced Composite Containing Penny-Shaped Crack in the Matrix," *J. Compos. Mater.*, **15**, 198-210 (1981).

[8].R.W.Davidge and T.J.Green, "The Strength of Two-Phase Ceramic/Glass Materials," *J. Mater. Sci.*, **3**, 629-634 (1968).

[9].J.A.Kuszky and R.C.Bradt, "Influence of Grain Size on Effects of Thermal Expansion Anisotropy in $MgTi_2O_5$," *J. Am. Ceram. Soc.*, **56** 420-423 (1973).

[10].J.A.Salem, Z.Li and R.C.Bradt, "Thermal Expansion and Elastic Anisotropy in Single Crystal Al_2O_3 and SiC Whiskers," in <u>Proc. of Symp. on Advances in Composite Materials and Structures</u>, Edited by S.S.Wang. ASM, Anaheim, CA, (1986).

[11].K.S.Mazdiyasni and L.M.Brown, "Synthesis and Mechanical Properties of Stoichiometric Aluminum Silicate (Mullite)," *J. Am. Ceram. Soc.*, **55**, 548-552 (1972).

[12].B.F.Backer and G.C.Wei, "Toughening Behavior in SiC-Whisker - Reinforced Alumina," *J. Am. Ceram. Soc.*, **67**, C267-C269 (1984).

[13].M.G.Jenkins, A.S.Kobayashi, K.W.White and R.C.Bradt, "Crack Initiation and Arrest in a SiC Whisker/Al_2O_3 Matrix Composite," *J. Am. Ceram. Soc.*, **70**, 393-395 (1987).

[14].P.Predecki, A.Abuhasan and C.S.Barrett, "Residual Stress determination in Al_2O_3/SiC (Whisker) Composites by X-Ray Diffraction," Advances in X-ray Analysis, 31 231-243 (1988).

[15]. A.Abuhasan, C.Balasingh and P.Predecki, "Residual Stresses in Alumina/Silicon Carbide (Whisker) Composites by X-ray Diffraction," *J. Am. Ceram. Soc.*, **73**, 2474-84 (1990).

[16].S.Majumdar, D.Kupperman and J.Singh, "Determination of Residual Thermal Stresses in a SiC-Al_2O_3 Composite Using Neutron Diffraction," *J. Am Ceram. Soc.*, **71**, 858-863 (1988).

[17].C.N.Tome, M.A.Bertinetti and S.R.MacEwen, "Correlation Between Neutron diffraction Measurements and Thermal Stresses in a Silicon Carbide/Alumina Composite," *J. Am. Ceram. Soc.*, **73** 3428-3432 (1990).

[18].T.Mah, M.G.Mendiratta and L.A.Boothe, "High Temperature Stability of Refractory Oxide-Oxide Composites," Technical Report **AFWAL-TR-88-4015** (1988).

[19]. Z.Li and R.C.Bradt, "Micromechanical Residual Stresses in SiC Whisker Reinforced Mullite Matrix and Si_3N_4 Matrix Composites," pp. 289-298 in Proc. Int. Conf. Whisker-and Fiber-Toughened Ceramics," Edited by R.A.Bradley, D.E.Clark, D.C.larsen and J.O.Stiegler, ASM International, Oak Ridge, Tennessee, (1988).

Table 1. Thermoelastic Properties of Reinforcing Phases and Matrices

Single Crystal Reinforcing Phase

	C_{11}	C_{33}	C_{12}	C_{13}	C_{44}	C_{14}	α_{11}	α_{33}
	(GPa)						$(10^{-6}/^{o}C)$	
β-SiC	352	352	140	140	233	---	4.45	4.45
Sapphire	497	499	164	112	147	-23.6	7.94	9.15

Polycrystalline Matrix

	E (GPa)	G (GPa)	ν	α $(10^{-6}/^{o}C)$
Alumina	402	169	0.23	8.34
Mullite	220	87.0	0.27	5.60

Figure Captions:

Fig. 1. Single Crystal Reinforcing Phase Inclusion in a Polycrystalline Ceramic Matrix.

Fig. 2. Residual Stresses within a Single SiC Reinforcing Inclusion as a Function of the (L/d) ratio in an Alumina Matrix Composite.

Fig. 3. Residual Stresses of SiC Whisker, (L/d)=10, as function of Volume Fraction, V_f for an Alumina Matrix Composite.

Fig. 4. Comparison of Residual Stresses between X-ray Measurement and Theoretical Calculation.

Fig. 5. Residual Stresses of 25% V_f C-type Sapphire Reinforcing Inclusion as a Function of the (L/d) Ratio in a Mullite Matrix Composite.

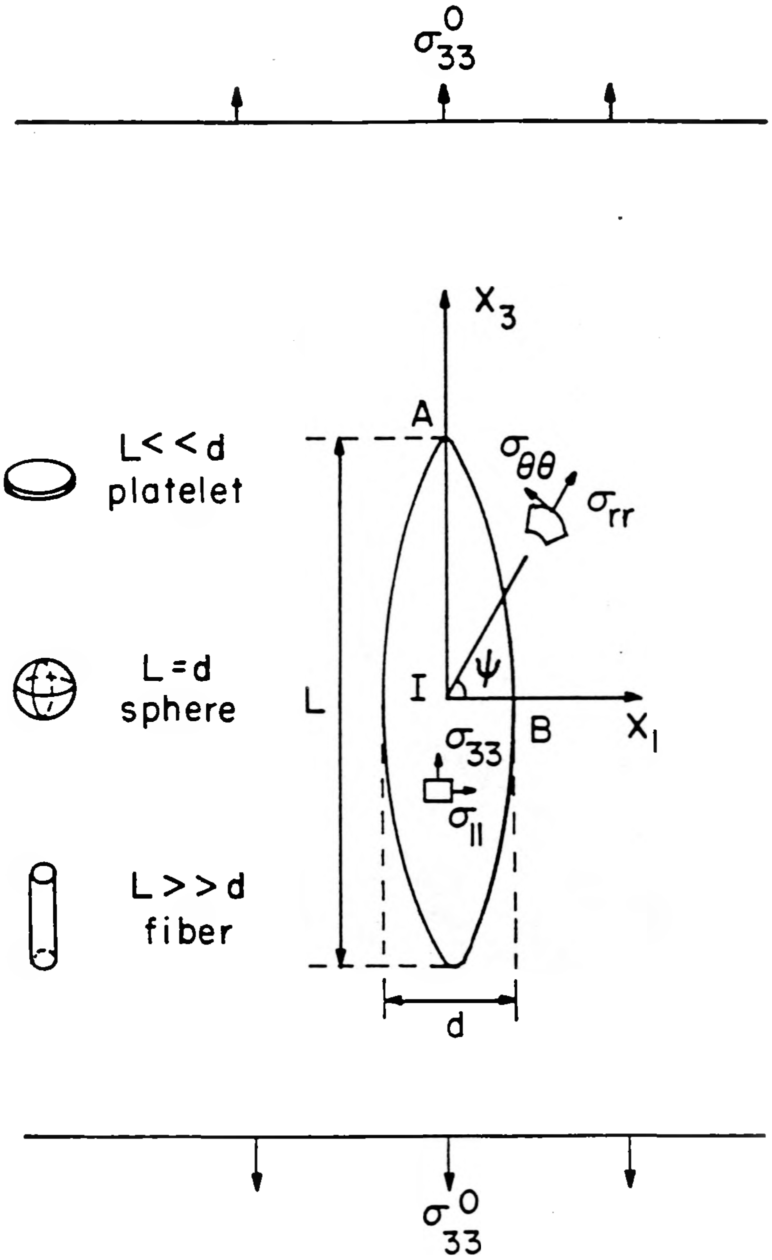

σ_{33}^{0}
X_3
A
$L<<d$
platelet
$\sigma_{\theta\theta}$
σ_{rr}
$L=d$
sphere
L
I
ψ
B
X_1
σ_{33}
σ_{11}
$L>>d$
fiber
d
σ_{33}^{0}

Fig. 1

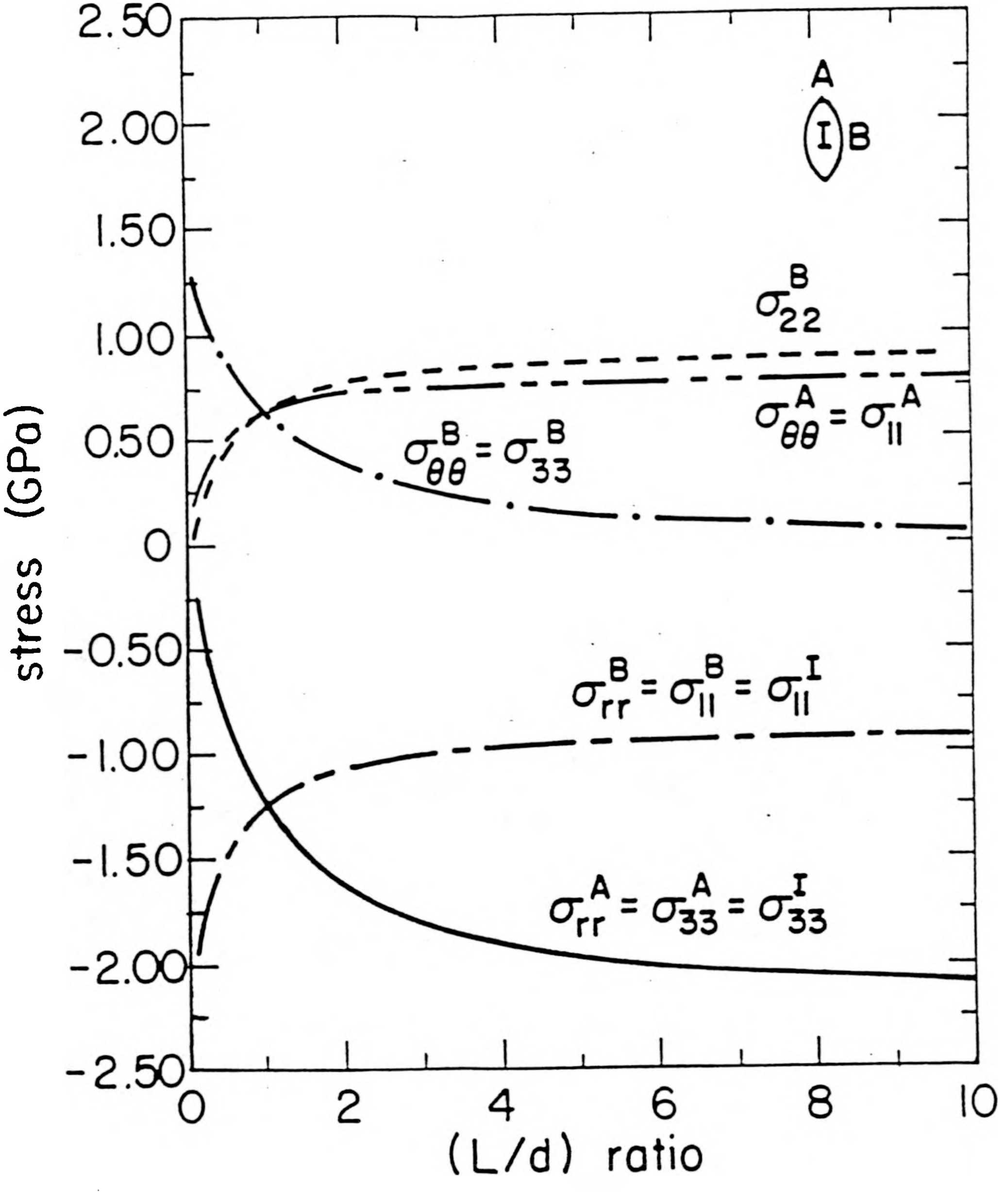
2.50
2.00
1.50
1.00
0.50
0
-0.50
-1.00
-1.50
-2.00
-2.50
0
2
4
6
8
10
stress (GPa)
(L/d) ratio
A
I
B
σ_{22}^{B}
$\sigma_{\theta\theta}^{A} = \sigma_{11}^{A}$
$\sigma_{\theta\theta}^{B} = \sigma_{33}^{B}$
$\sigma_{rr}^{B} = \sigma_{11}^{B} = \sigma_{11}^{I}$
$\sigma_{rr}^{A} = \sigma_{33}^{A} = \sigma_{33}^{I}$

Fig. 2

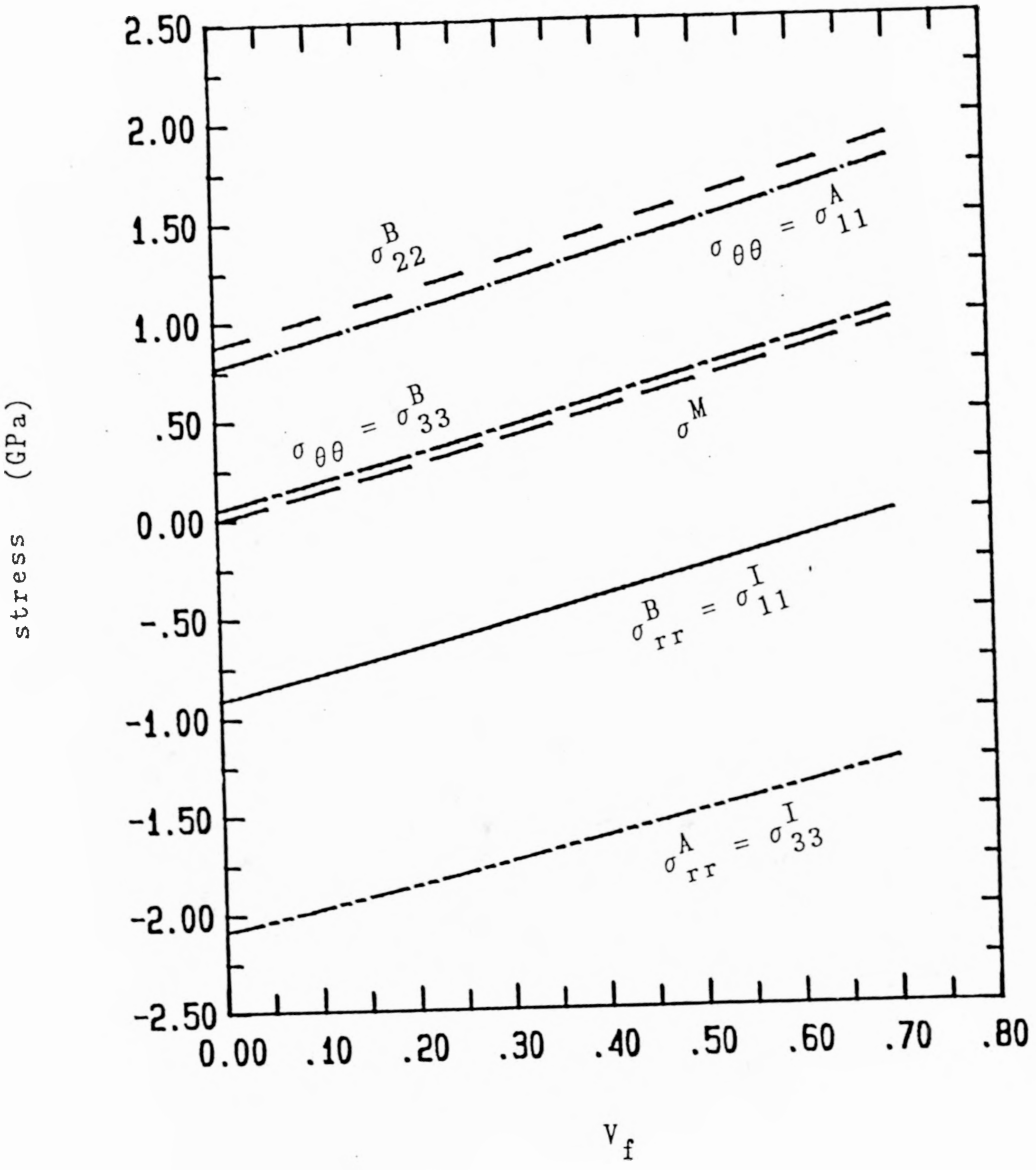
2.50
2.00
1.50
1.00
.50
0.00
-.50
-1.00
-1.50
-2.00
-2.50
stress (GPa)
0.00
.10
.20
.30
.40
.50
.60
.70
.80
V_f
σ^B_{22}
$\sigma_{\theta\theta} = \sigma^A_{11}$
$\sigma_{\theta\theta} = \sigma^B_{33}$
σ^M
$\sigma^B_{rr} = \sigma^I_{11}$
$\sigma^A_{rr} = \sigma^I_{33}$

Fig. 3

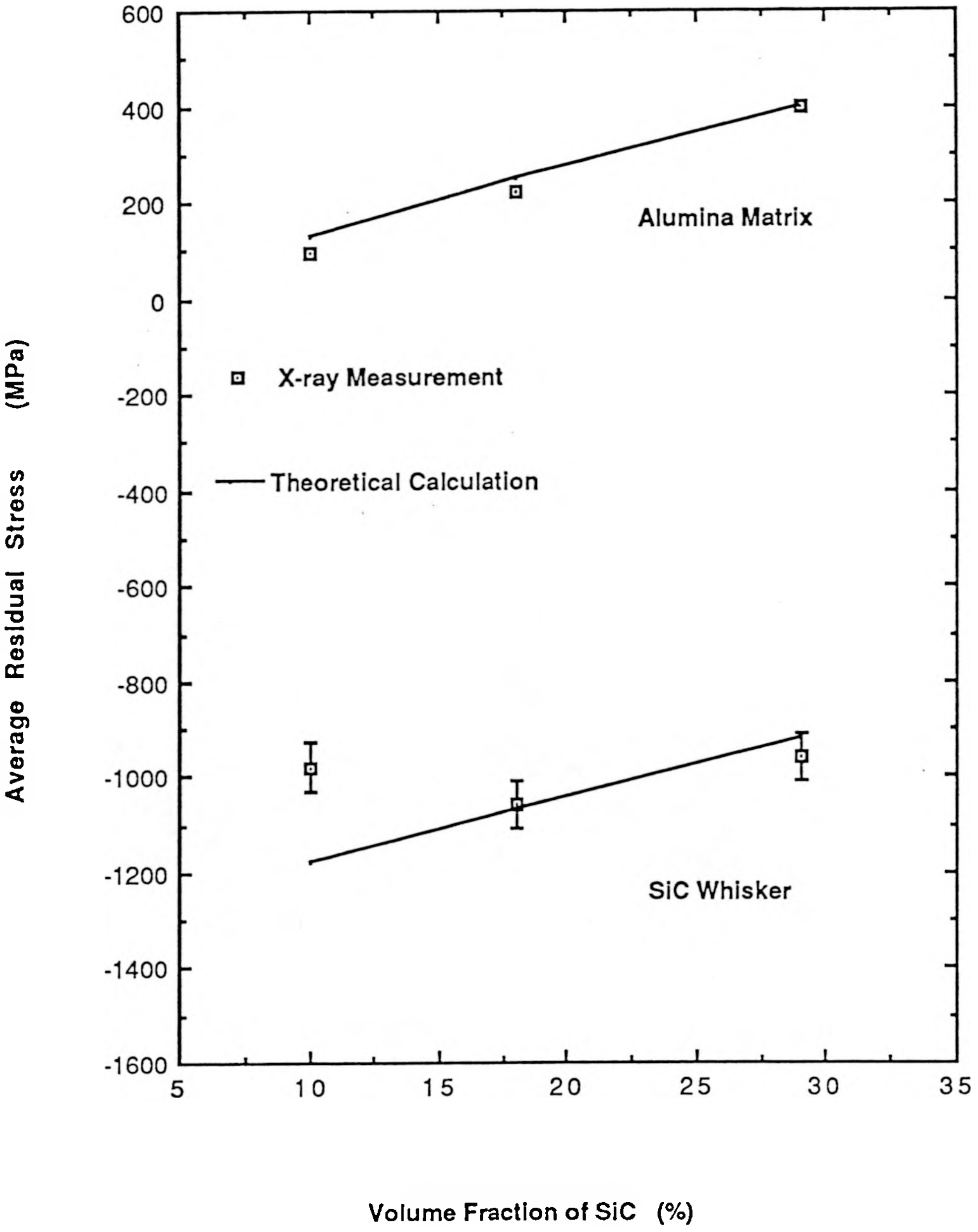
600
400
200
0
-200
-400
-600
-800
-1000
-1200
-1400
-1600
5
10
15
20
25
30
35
Average Residual Stress (MPa)
Volume Fraction of SiC (%)
Alumina Matrix
SiC Whisker
X-ray Measurement
Theoretical Calculation

Fig. 4

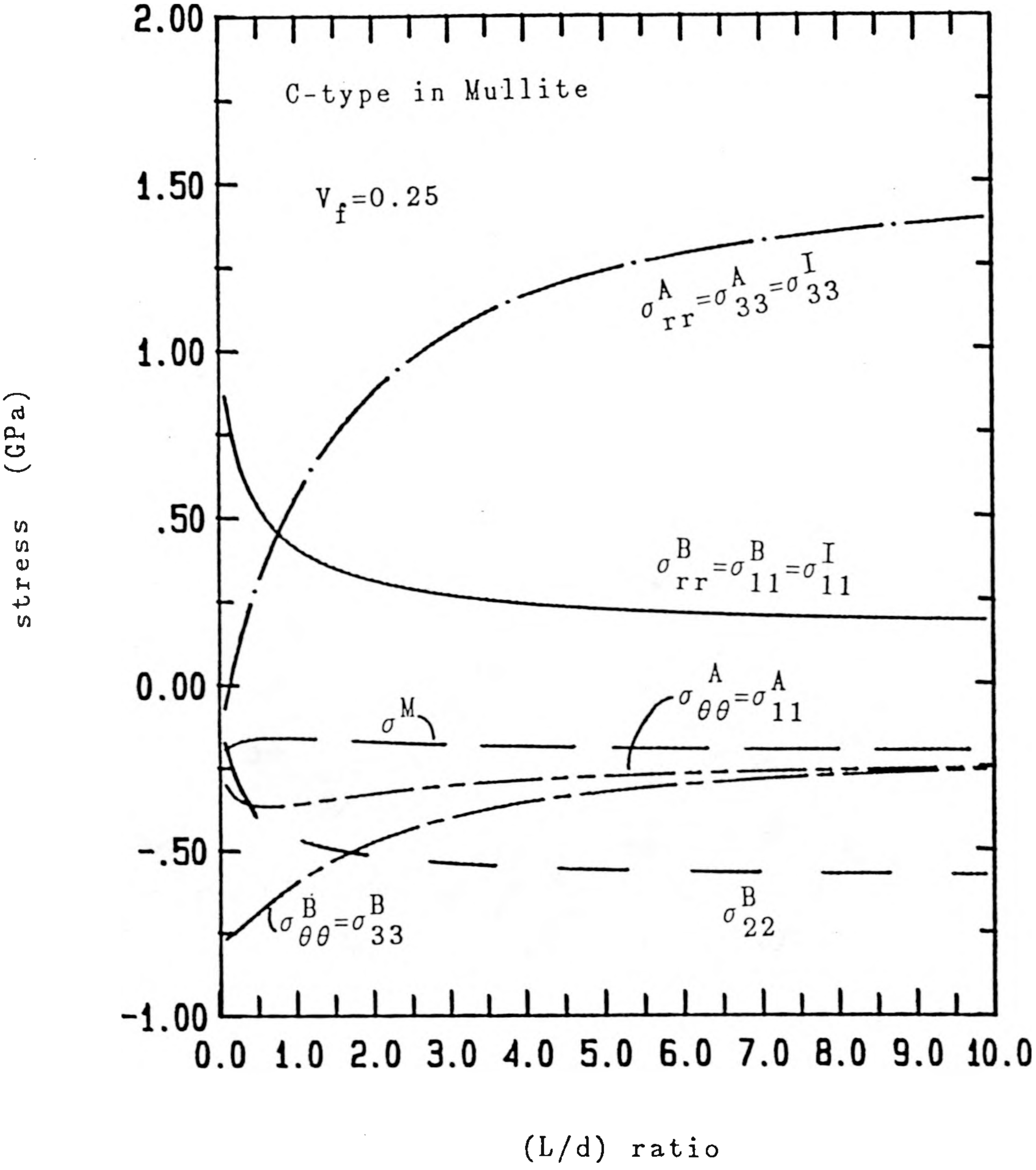
C-type in Mullite
$V_f=0.25$
$\sigma^A_{rr}=\sigma^A_{33}=\sigma^I_{33}$
$\sigma^B_{rr}=\sigma^B_{11}=\sigma^I_{11}$
σ^M
$\sigma^A_{\theta\theta}=\sigma^A_{11}$
$\sigma^B_{\theta\theta}=\sigma^B_{33}$
σ^B_{22}
2.00
1.50
1.00
.50
0.00
-.50
-1.00
0.0
1.0
2.0
3.0
4.0
5.0
6.0
7.0
8.0
9.0
10.0
stress (GPa)
(L/d) ratio

Fig. 5